Hindawi
Mathematical Problems in Engineering
Volume 2019, Article ID 1752803, 14 pages
https://doi.org/10.1155/2019/1752803

Research Article

Proximity Effects on Characteristics of Flow around Three Inline Square Cylinders

Waqas Sarwar Abbasi,[1] **Shams Ul Islam**,[2] **and Hamid Rahman**[3]

[1]*Mathematics Department, Air University, Islamabad, 44000, Pakistan*
[2]*Mathematics Department, COMSATS Institute of Information Technology Islamabad, 44000, Pakistan*
[3]*Mathematics and Statistics Department, Bacha Khan University, Charsadda, 44000, Pakistan*

Correspondence should be addressed to Waqas Sarwar Abbasi; waqas-555@hotmail.com

Received 20 August 2018; Accepted 18 December 2018; Published 10 January 2019

Academic Editor: Sergey A. Suslov

This work presents the numerical investigations performed to study the proximity effects on fluid flow characteristics around three inline square cylinders using the lattice Boltzmann method. For this purpose the gap spacing (g) is systematically varied in the range 0.5 to 16 diameters of cylinder by keeping Reynolds number fixed at 200. Five different flow patterns are observed at different values of spacing: bluff body flow, gap trapped flow, irregular flow, alternate shedding, and modulated shedding. These patterns have a significant effect on flow induced forces and vortex shedding frequency. The spacing value $g = 2$ is found to be critical due to sudden changes in fluid flow characteristics. The flow parameters of first cylinder are found to be closer to single cylinder values but for middle and third cylinder the differences confirm the wake interference effect even at large values of spacing.

1. Introduction

Numerical analysis of the problems concerning interaction of fluid with solid structures has received increasing attention recently because of its wider applications in real life, industrial and engineering problems. Examples can be found in many areas such as aircraft, heat exchanger tubes, cooling systems for nuclear power plants, transmission cables, bridges, high rise buildings, and electronic equipment. Similarly at low Reynolds numbers these applications can be found in microelectromechanical systems (MEMS) and cooling of fibers. Square cylinder serves as a basic component in the design of such structures. These structures often interact with fluids like air or water and experience flow induced forces which can lead to their failure under certain unfavorable circumstances. Therefore it is important to fully understand these interactions and their resulting effects on the structures in order to improve the structural designs and also to avoid industrial loss.

When one cylinder is immersed in the wake of another, the fluid flow characteristics strongly depend on the gap spacing (g) between cylinders, geometric parameters related to cylinders arrangement, Reynolds number (Re), and shape of the cylinders [1–4]. Despite numerous investigations of the flow patterns and force coefficients of the flow past circular cylinders, very little attention has been directed toward the flow interference effects around an inline array of square cylinders [5–10]. The main difference between circular and square cylinder geometry is the point of separation of flow. In case of former one it is not fixed while for the latter one it is fixed [11]. This alters the flow interference effects considerably. Also the characteristics of flow are different for different shapes of cylinders like circular, square, and rectangular [12–14]. Further, the flow interference effects also change with different arrangements of cylinders even at the same values of spacing and Re [15].

Very few experimental and numerical studies have been carried out for the flow around inline arranged square cylinders. Some representative experimental studies are those of Kim et al. [16], Liu and Chen [17], Sakamoto et al. [18], Sayers [19], and Lam and Lo [20]. Kim et al. [16] experimentally

measured the flow fields around two square cylinders in a tandem (inline) arrangement. Their results showed that the flow patterns at gap spacing $g \leq 2$ were drastically different from those at $g \geq 2.5$. Liu and Chen [17] observed two different kinds of flow patterns by progressively increasing and decreasing the gap spacing, from 1.5 to 9, between two tandem square cylinders. Sakamoto et al. [18] experimentally observed significant changes in time-averaged forces of square cylinders for gap spacing above and below $g = 4$ at $Re = 27{,}600$. Sayers [19] measured the lift coefficient (CL) and drag coefficient (CD) of a single cylinder in a group of four equally spaced cylinders placed in an open-jet wind tunnel. Lam and Lo [20] reported three different kinds of behaviors of shear layers while investigating the flow around four inline cylinders. While searching the literature, it can be observed that most of the experimental results are limited to high values of Re and less information is available about the phenomena of low Re regarding the experimental studies. On the other hand, numerical techniques are capable of capturing the flow characteristics at both high and low values of Re efficiently. Inoue et al. [21] numerically examined the sound generation in a uniform flow at low Mach number (Ma) and Re for flow past two inline square cylinders. Etminan [22] numerically investigated the fluid flow and heat transfer for flow past square cylinders at $1 \leq Re \leq 200$ and Prandtl number $Pr = 0.71$. Their results showed that the flow was steady for $Re \leq 35$ and unsteady-periodic for $Re \geq 40$. Bao et al. [23] investigated the flow past an inline array of six square cylinders at $Re = 100$ and g ranging from 1.5 to 15. They observed six different kinds of flow patterns: steady wake, non-fully developed vortex street in single-row and double-row, fully developed vortex street in double-row, fully developed vortex street in partially recovered single-row, and fully developed multiple vortex streets. They also observed that the first and second cylinder behave similar to the two inline cylinders configuration in terms of aerodynamic force coefficients while the other four cylinders experience periodic variation of forces with the increase in gap spacing. For more details about fluid flow from an inline array of cylinders, interested readers are referred to [24–26] and references therein.

In the present study, the case of flow interacting with an inline array of three square cylinders is considered, because inline array of cylinders is a fundamental element in any tube array, offshore structures, and microelectromechanical system (MEMS) devices. In this work special attention is paid to the investigation of the characteristics of vortex shedding and flow induced forces caused by the flow interference of multiple cylinders. We will mainly focus on the existence of different flow patterns under the effect of g by fixing Re at a specific value, dependence of force coefficients on g, and existence of critical spacing values (if any) where flow characteristics change abruptly.

2. Lattice Boltzmann Method

Lattice Boltzmann method, evolved from lattice gas cellular automata (LGCA) [27], was firstly introduced by McNamara and Zanetti [28]. The lattice Boltzmann evaluation equation with Bhatnagar-Gross-Krook collision model [29] is defined as

$$f_i\left(\boldsymbol{x} + \boldsymbol{e}_i \Delta t, t + \Delta t\right) = f_i\left(\boldsymbol{x}, t\right) - \frac{1}{\tau}\left(f_i\left(\boldsymbol{x}, t\right) - f_i^{(eq)}\left(\boldsymbol{x}, t\right)\right) \tag{1}$$

where f_i is particle distribution function along the particle speed direction $\boldsymbol{e}_i$ at position $\boldsymbol{x}$ and time t. $f_i^{(eq)}$ denotes the equilibrium distribution function and τ is the single relaxation time parameter.

The macroscopic velocity $\boldsymbol{u}$ and density ρ are calculated by the following relations.

$$\rho = \sum_{\boldsymbol{i}} f_i, \qquad \boldsymbol{u} = \frac{1}{\rho}\sum_{\boldsymbol{i}} f_i \boldsymbol{e}_i \tag{2}$$

The equilibrium distribution function depending on density and velocity is given as [30]

$$f_i^{(eq)} = \omega_i \rho \left[1 + \frac{3}{c^2}\boldsymbol{e}_i.\boldsymbol{u} + \frac{3}{2c^4}\left(\boldsymbol{e}_i.\boldsymbol{u}\right)^2 - \frac{3}{2c^2}\boldsymbol{u}.\boldsymbol{u}\right] \tag{3}$$

where $c = \Delta \boldsymbol{x}/\Delta t$ is the lattice speed while $\Delta \boldsymbol{x}$ and Δt are the lattice width and time step, respectively. In the present work $\Delta \boldsymbol{x} = \Delta t$ which means that $c = 1$. The weighting factors ω_i for the two-dimensional and nine-velocity particle (D_2Q_9) model [30], considered in the present study, are $\omega_0 = 4/9$, $\omega_{i=1,2,3,4} = 1/9$, and $\omega_{i=5,6,7,8} = 1/36$. Furthermore, the speed of sound is $c_s = c/\sqrt{3}$ and the kinematic viscosity is taken to be $\nu = (\tau - 1/2)c_s^2 \Delta t$. Further details about LBM can be found in [31].

3. Geometry of Problem

The schematic flow diagram for the problem under consideration is given in Figure 1. Three square cylinders having the same size (d) are placed, inline to each other, inside a rectangular domain of length L and height H. The first cylinder (c_1) is placed at a distance $L_u = 6$ from the entrance of computational domain. The second cylinder (c_2) is placed at a gap distance g from c_1 while the third cylinder (c_3) is also placed at a gap distance g from c_2. Similarly the distance from c_3 to the exit position of computational domain is $L_d = 25$. All the lengths are nondimensionalized using the cylinder size "d". Uniform inflow condition ($u = U_\infty$ and $v = 0$) is incorporated at entrance of computational domain. While at exit position, convective boundary condition ($\partial_t u + U_\infty \partial_x u = 0$) is applied in terms of distribution functions [32]. At solid surfaces, including the surface of cylinders and walls of channel, the bounce back rule is applied which resembles to the no-slip boundary condition [33].

For the sake of brevity we are not giving details about grid independence, domain independence, and code validation study. These details can be found in our recently published articles [10, 24, 26].

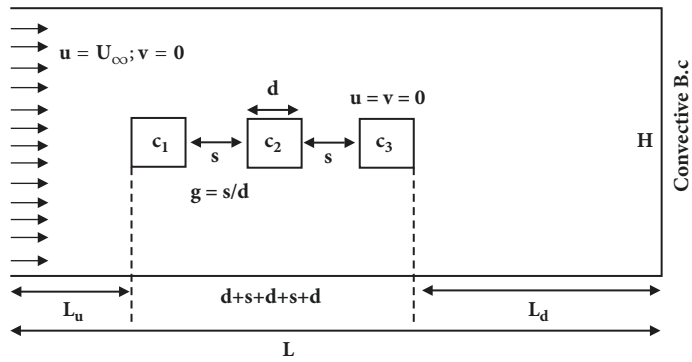

Figure 1: Schematic flow diagram.

4. Results and Discussion

It is clear from previous investigations that in fluid-structure interaction problems, the behavior of flow around cylinders depends on the shape, size, and number of cylinders in the flow field [1]. Compared to other arrangements the flow behavior around a triad has gained very little attention although this geometry is of practical relevance. Keeping in view these observations, the present study is conducted to analyze the flow behavior around three inline square cylinders under the effect of gap spacing, ranging from 0.5 to 16, at a fixed value of $Re = 200$. Our main aim is to observe the dependence of flow structure and force variation on spacing between cylinders. The reason for fixing Re at 200 is that at such Re, the flow becomes fully developed and vortices are generated in the flow field regardless of the number of cylinders and gap spacing.

In this work the spacing between cylinders is systematically altered from lower to higher values. The flow structure is divided into different patterns depending on vortex generation mechanism and forces variation. In the following subsections these flow patterns are discussed in detail.

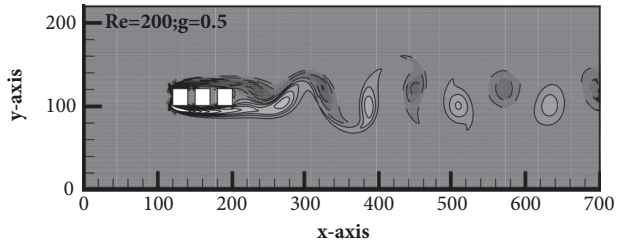

Figure 2: Vorticity contour for bluff body flow.

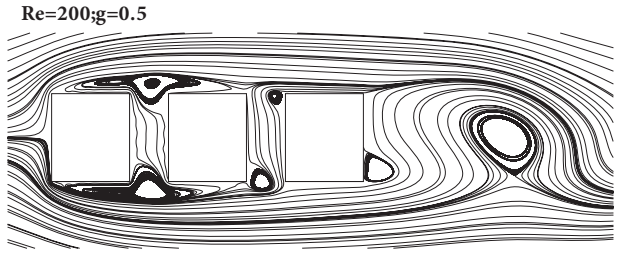

Figure 3: Streamlines visualization for bluff body flow.

4.1. Flow Patterns

4.1.1. Bluff Body Flow. Bluff body flow pattern is seen in this study for the spacing range 0.5 to 1. A representative case for this flow pattern is shown in Figure 2 at $g = 0.5$. In this pattern, the famous Karman vortex street appears in the wake of third cylinder only. All bodies in the flow field behave like a solo body. Main reason for such pattern is that the close proximity prevents entering of flow within the gaps between cylinders. Similar flow pattern was also observed by Igarashi and Suzuki [34] for three inline circular cylinders at $g = 1.32$. According to them this flow pattern normally occurs when Re is less than a critical value. In this flow pattern shear layers from first cylinder do not reattach and vortices rotate in clockwise as well as counterclockwise fashion at downstream wake region only (Figure 2). Streamlines visualization of this flow pattern is presented in Figure 3. The transverse oscillations of streamlines in the wake of third cylinder are due to vortex formation. Small recirculating vortices appear at corners of cylinders but diffuse quickly due to narrow space between bodies and become apparent in the wake of third cylinder only. Zdravkovich [1] classified such type of flow pattern as single slender body.

Figure 4 shows the temporal variation of drag and lift coefficients of triad. From Figure 4(a) it can be observed that a constant drag force is exerted by fluid on all cylinders. Due to small spacing, shear layers cannot enter within the gaps between cylinders which restrict variation in drag force. Also the first cylinder in triad experiences highest drag force while the middle one experiences lowest drag force. This is due to the fact that the middle cylinder is shielded by both upstream and downstream cylinder. Similar observation about drag force was reported by Zadrakovich [1] for three inline circular pipes at spacing values 1.5 and 2. Furthermore, due to vortex generation phenomenon, the lift coefficient

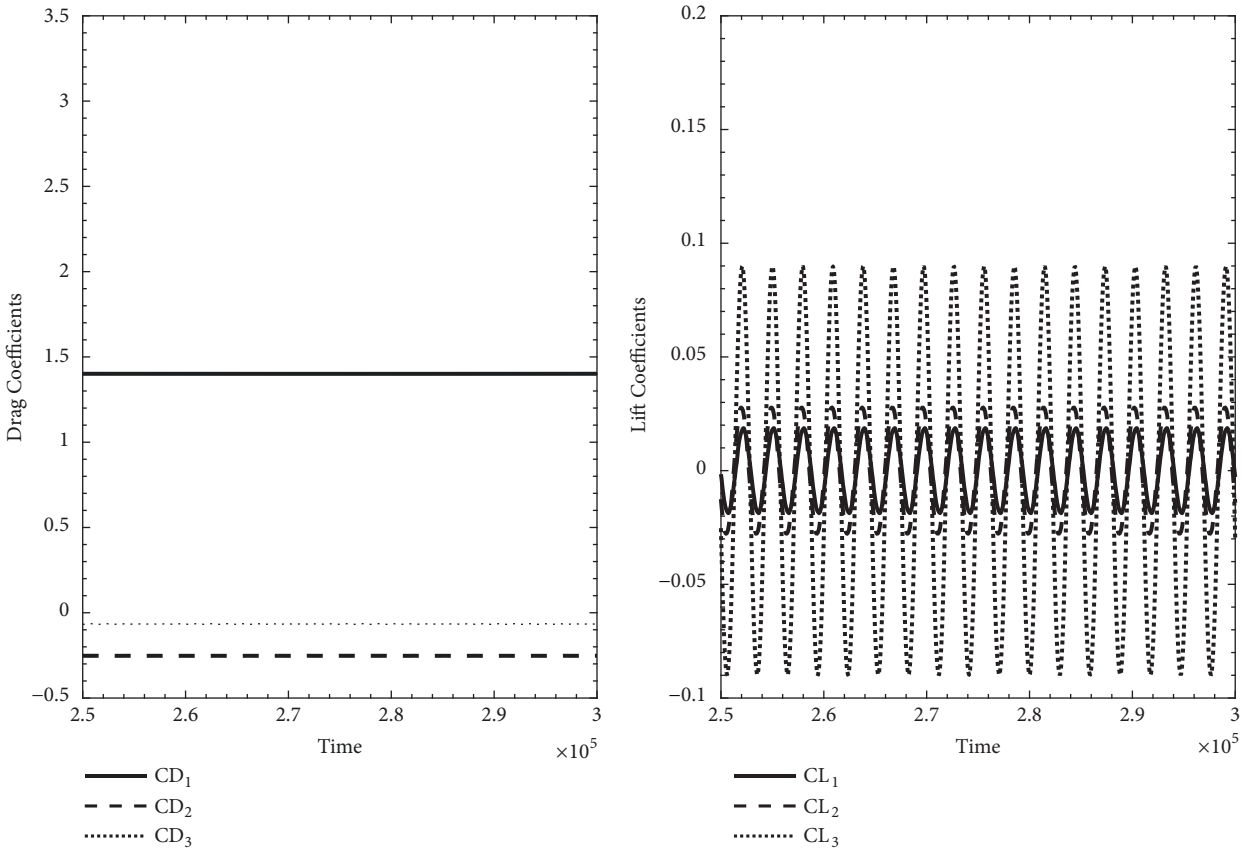

(a) Re = 200; g = 0.5 (b) Re = 200; g = 0.5

Figure 4: Temporal variation of force coefficients for bluff body flow.

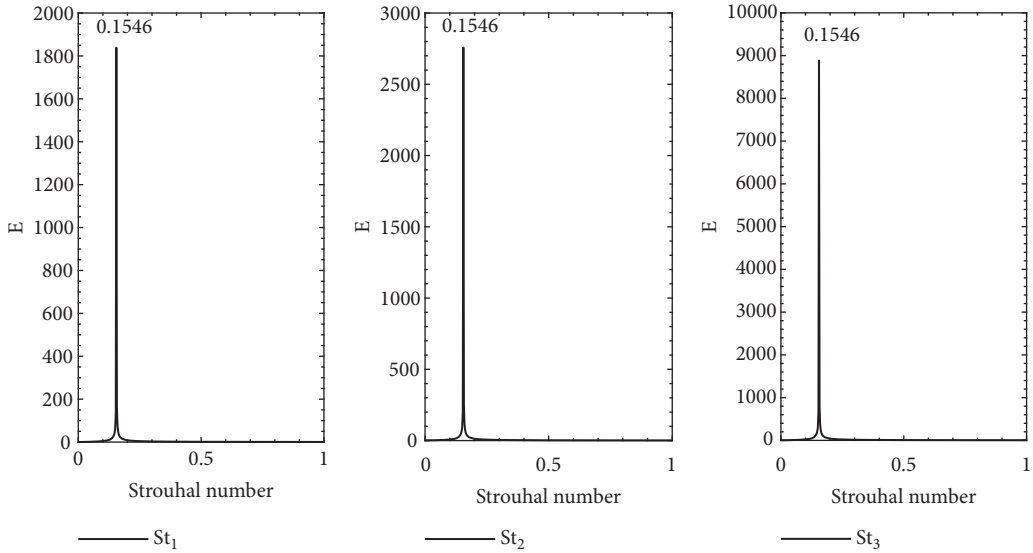

(a) Re = 200; g = 0.5 (b) Re = 200; g = 0.5 (c) Re = 200; g = 0.5

Figure 5: Power spectrum graph for bluff body flow.

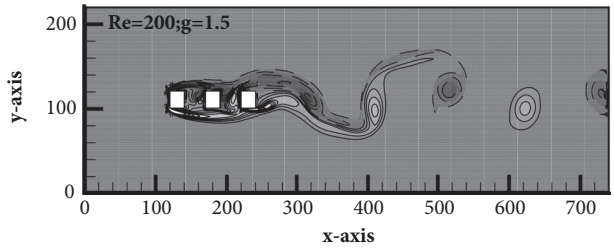

Figure 6: Vorticity contour for gap trapped flow.

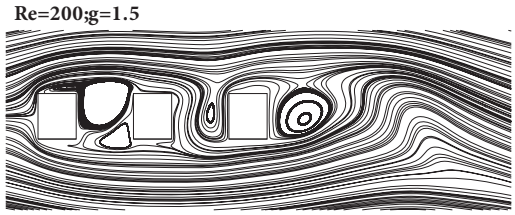

Figure 7: Streamlines visualization for gap trapped flow.

of all cylinders varies periodically (Figure 4(b)). And since vortex shedding occurs behind last cylinder, the amplitude of lift cycles for c_3 is higher than other upstream cylinders. The power spectrum graph for bluff body flow pattern shows a single peak for all cylinders in triad (Figure 5). This is due to the fact that the flow moves smoothly in the whole domain without any disturbance, which ensures the existence of a single frequency which is vortex shedding frequency.

4.1.2. Gap Trapped Flow. Gap trapped flow pattern is observed in this study at the spacing value $g = 1.5$. Vorticity contour for this flow pattern is presented in Figure 6. In this flow pattern the shear layers detaching from upstream cylinders merge within the gaps between cylinders due to slight increment in spacing. But the insignificant space restricts the rollup of these shear layers to form vortices; instead the flow is trapped between gaps. At downstream wake region the vortices circulate at lager region as compared to bluff body flow. The streamlines for this flow pattern show waviness within the gaps as well as in the wake region of c_3 also (Figure 7). Hetz et al. [35] named such flow pattern as cavity shedding. Sewatkar et al. [36] also observed such flow around six inline cylinders and named it as quasi periodic flow. Zdravkovich [1] named this type of flow pattern as quasi steady reattachment.

The temporal variation of drag coefficient shows that, unlike bluff body pattern, the drag coefficient of all cylinders transversally oscillates with smaller amplitude cycles and is no more constant (Figure 8(a)). This is due to movement of flow within the gaps. Also the amplitude of lift cycles is increased in this flow pattern (Figure 8(b)). This is due to the circulation of vortices at larger region as compared to bluff body flow pattern. And due to larger recirculation zone the spectrum energy of all cylinders in triad also increased (Figure 9).

4.1.3. Irregular Flow. Another flow pattern observed in this study is irregular flow. This type of flow structure occurred in the spacing range $g = 2$ to 2.5. A representative case of vorticity contour for irregular flow is shown in Figure 10 at $g = 2$. It can be observed that the shear layers exhibit complex amalgamation and distortion behavior after interacting with second cylinder. This complexity becomes more prominent in the wake region of third cylinder. The Karman vortex street, observed in the previous two flow patterns, no more ensues. Due to chaosity in flow structure the streamlines exhibit wavelike variation in the whole computational domain behind first cylinder contrary to that observed in bluff body and gap trapped flow patterns (Figure 11). Also the streamlines, from one side, crossover the other sides of cylinders. Furthermore, the amplitudes of drag as well as lift coefficients of c_2 and c_3 are modulated (Figure 12). This indicates that the flow exerts higher magnitude unsteady forces on second and third cylinders. The spectrum graphs show multiple peaks due to impingement of flow (Figure 13). The diffused peaks become more apparent for second and third cylinders. These smaller diffused peaks in spectrum graphs indicate the effect of secondary frequencies due to complexity in flow structure. Zdravkovich [1] named such flow pattern as intermittent shedding. Sewatkar et al. [36] also observed such flow pattern for six inline square cylinders at $Re = 100$ and for $g \geq 6$ and named it as chaotic flow. According to Patil and Tiwari [9] at $g = 2$ and $Re = 150$ vortex shedding is completely absent for two-inline-cylinder case while at $g = 3$ and 4 vortex shedding starts in the wake of second cylinder.

4.1.4. Alternate Shedding. When the spacing between cylinders increases, vortices start shedding from each component of triad. A representative case of vorticity contour for this flow pattern is shown in Figure 14 at $g = 3$. The shape and size of generated vortices, in the wake of third cylinder, are completely different from those observed in previous flow patterns. These vortices shed alternately from each cylinder. The vortices shedding from first cylinder initially impinge with second and then with third cylinder, respectively. These vortices travel in a smooth fashion exhibiting the Karman vortex street. Due to this behavior the flow pattern is named as alternate shedding. The reason behind this type of flow structure is that with increment in spacing there is enough room for complete development of vortices. The variation of streamlines within the gaps as well as at downstream wake region also confirms the alternate shedding pattern (Figure 15). The lift coefficients of all cylinders transversely oscillate with higher amplitude as compared to previous flow patterns (Figure 16(b)). The power spectrum graph indicates the existence of a single frequency which is vortex shedding frequency (Figure 17). This type of flow pattern was also observed by Harichandan and Roy [15] for flow around three inline circular cylinders at $g = 5$. According to them at $g = 5$ the Karman vortex street develops behind each

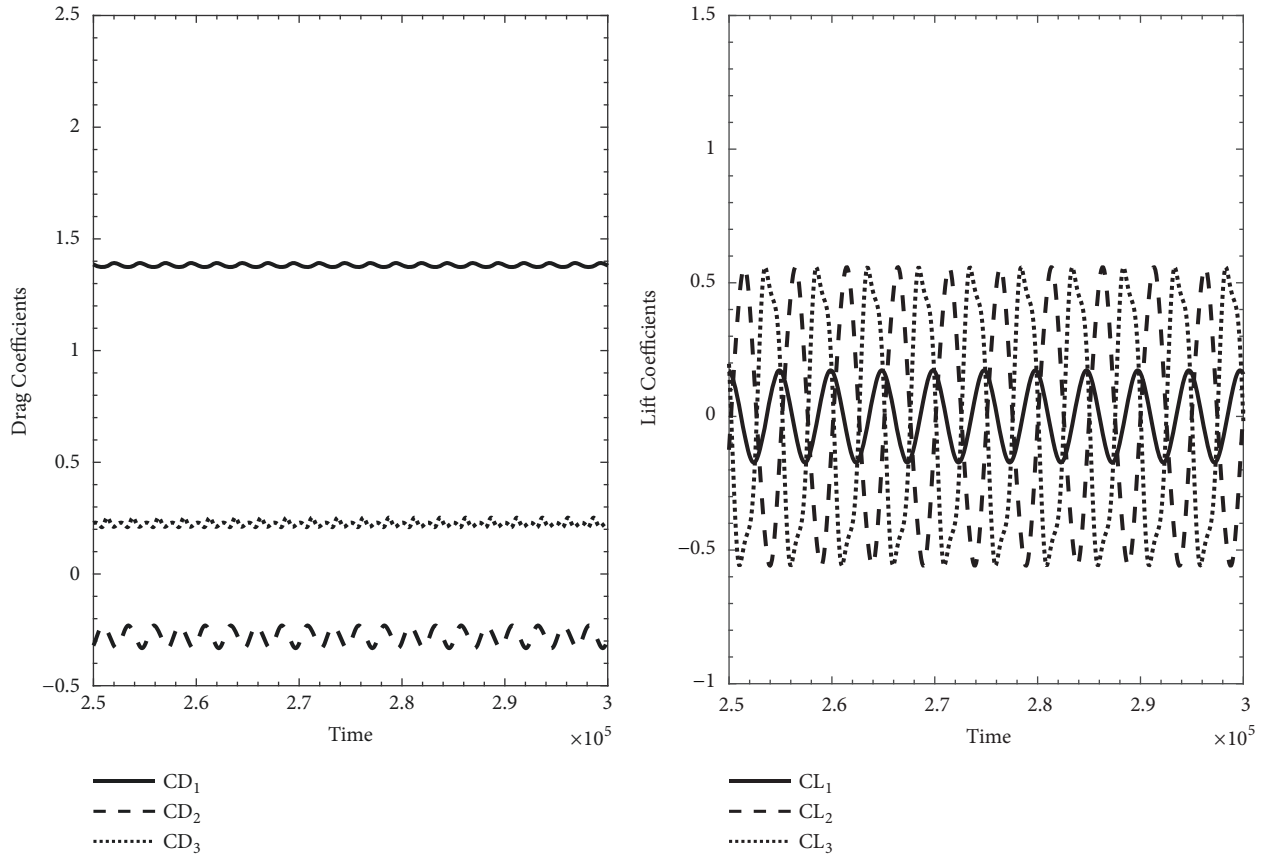

(a) Re = 200; g = 1.5 (b) Re = 200; g = 1.5

Figure 8: Temporal variation of force coefficients for gap trapped flow.

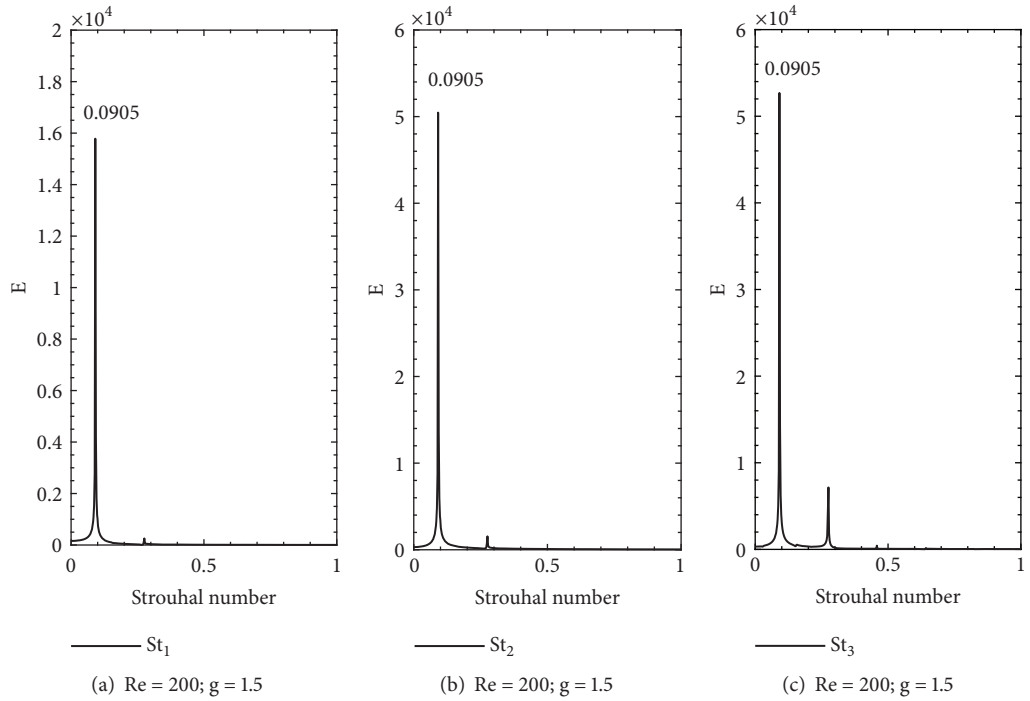

(a) Re = 200; g = 1.5 (b) Re = 200; g = 1.5 (c) Re = 200; g = 1.5

Figure 9: Power spectrum graph for gap trapped flow.

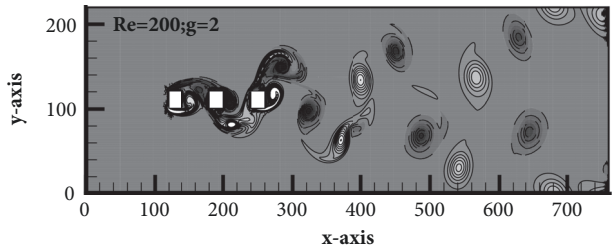

Figure 10: Vorticity contour for irregular flow.

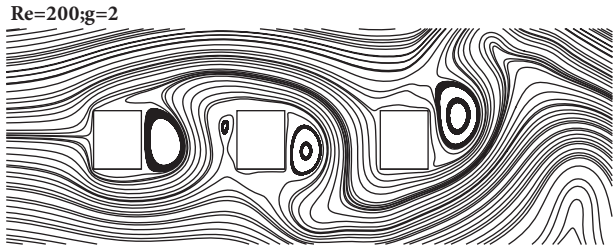

Figure 11: Streamlines visualization for irregular flow.

cylinder and the vortex shedding from downstream cylinder is disturbed due to impingement of vortex streets emerging from upstream cylinders. Hetz et al. [35] named this type of flow structure as gap shedding in the case of five inline cylinders. According to Deng et al. [6] vortex shedding does not take place between two inline circular cylinders for $g \leq 3.5$ and $Re = 220$. Also the results of Inoue et al. [21] revealed that, for two inline square cylinders case at $Re = 150$, the rollup of shear layers separated from upstream cylinder is suppressed for $g < 3.5$, while for $g > 3.5$ shear layers roll up to form vortices in the wake of both cylinders. Bao et al. [23] reported that at $Re = 100$ and $g = 3$ the wake is steady for six-inline-cylinder case. It is important to mention here that the alternate shedding flow pattern occurs for the spacing range $g = 3$ to 6.

4.1.5. Modulated Shedding. When gap spacing further increases, the Karman vortex street completely develops in first gap (Figures 18(a) and 18(b)). The clockwise and counterclockwise vortices can be clearly distinguished. But after impingement with second cylinder the complexity appears in flow structure. The regularity of clockwise and counterclockwise vortices disappears. This phenomenon also holds in the wake of third cylinder. The streamlines also indicate the formation of Karman vortex street in first gap but after that modulation appears (Figures 19(a) and 19(b)). Due to these characteristics the follow pattern is named as modulated shedding and it is observed in the spacing range $8 \leq g \leq 16$. The drag and lift coefficients for this flow pattern are shown in Figure 20. The effect of intonation in flow structure can be seen in the drag coefficients of second and third cylinder (Figures 20(a) and 20(c)). The lift coefficients of all cylinders are in periodic steady state due to which a single peak appears in the power spectrum graphs of all cylinders (Figures 20(b), 20(d), and 21). Bao et al. [23] observed this type of flow for six inline cylinders and named it as non-fully developed single-row vortex street. Zdravkovich [1] classified this type of flow pattern as binary vortex street for two inline cylinders and concluded that the flow regimes for two inline cylinders may also occur for case of three cylinders but within different range of spacing and in modified form.

Figure 22 represents a complete picture of flow patterns observed in this study at different spacing values. Since we have considered three cylinders geometry, there are two gap ratios: first gap ratio between first and second cylinder and second gap ratio between second and third cylinder. The first gap ratio is plotted along x-axis while the second gap ratio along y-axis. It can be observed from this figure that the gap trapped flow occurred at only one spacing value, while the alternate shedding and modulated alternate shedding flow patterns are the mostly seen flow patterns.

4.2. Force Statistics. Dependence of different flow parameters, like average drag coefficient (CD_{MEAN}), Strouhal number (St), and root-mean-square (RMS) values of CD and CL of all cylinders in triad, on gap spacing is shown in Figure 23. The single cylinder values are also plotted for comparison. Figure 23(a) shows that the CD_{MEAN} of first cylinder is closer to that of single cylinder values at all spacing values. It is slightly less than the single cylinder value till $g = 1.5$. But after that it coincides with the single cylinder CD_{MEAN}. It should be noted that after $g = 1.5$ the flow pattern changes from gap trapped to irregular and vortex shedding starts within the gaps also. The CD_{MEAN} of second cylinder is negative till $g = 1.5$ and at $g = 2$ it jumps to positive values which shows that $g = 2$ is drag inversion spacing. The negative values of drag force indicate that due to strong suction effect, within the gaps, the drag force acts like thrust force. After $g = 2.5$ the CD_{MEAN} of second cylinder slightly decreases/increases due to the fact that after $g = 2.5$ the vortex generation starts from each cylinder (see Figures 14 and 18). According to results of Zdravkovich [1] for circular cylinders, at smaller spacing values, the middle cylinder experiences less drag force as compared to side ones while reverse trend occurs for higher spacing values. Here in our case the CD_{MEAN} of middle cylinder is less than that of third cylinder till $g = 2.5$ but after that reverse trend arises. The highest value of CD_{MEAN} is that of third cylinder attained at $g = 2.5$. It is important to mention that at $g = 2.5$ the irregular flow pattern was observed (see Figure 22). Also Figure 23(a) shows that at g = 2 and 2.5 the CD_{MEAN} of both downstream cylinders is relatively high as compared to other spacing values, which indicates that, in irregular flow pattern, fluid exerts high magnitude drag force on cylinders.

Figure 23(b) shows St as a function of gap spacing. It can be seen that the St of all cylinders is the same at a particular spacing value. This indicates the fact that at all spacing values, considered in this study, the vortex shedding frequency is dominant even for the irregular flow pattern where complex flow structure was observed (see Figure 10).

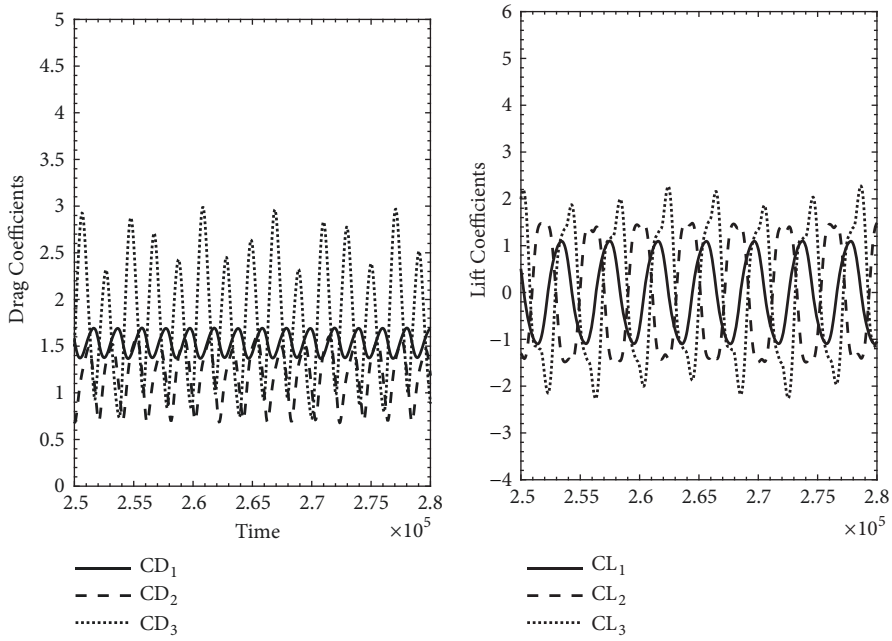

(a) Re = 200; g = 2 (b) Re = 200; g = 2

Figure 12: Temporal variation of force coefficients for irregular flow.

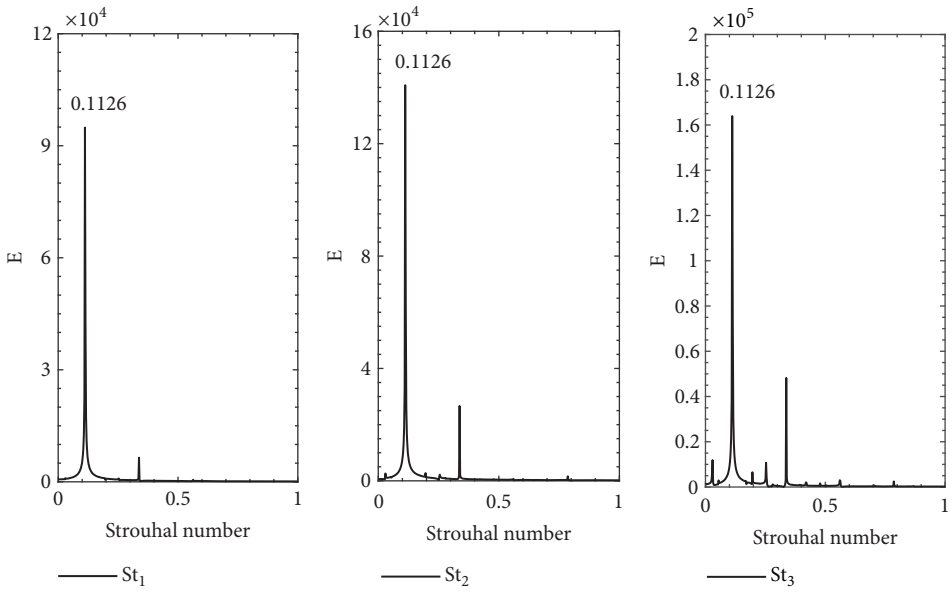

(a) Re = 200; g = 2 (b) Re = 200; g = 2 (c) Re = 200; g = 2

Figure 13: Power spectrum graph for irregular flow.

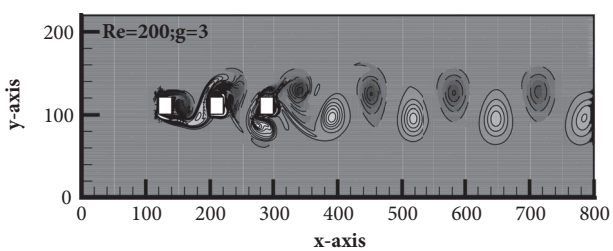

Figure 14: Vorticity contour for alternate shedding.

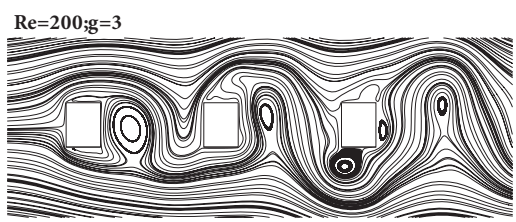

Figure 15: Streamlines visualization for alternate shedding.

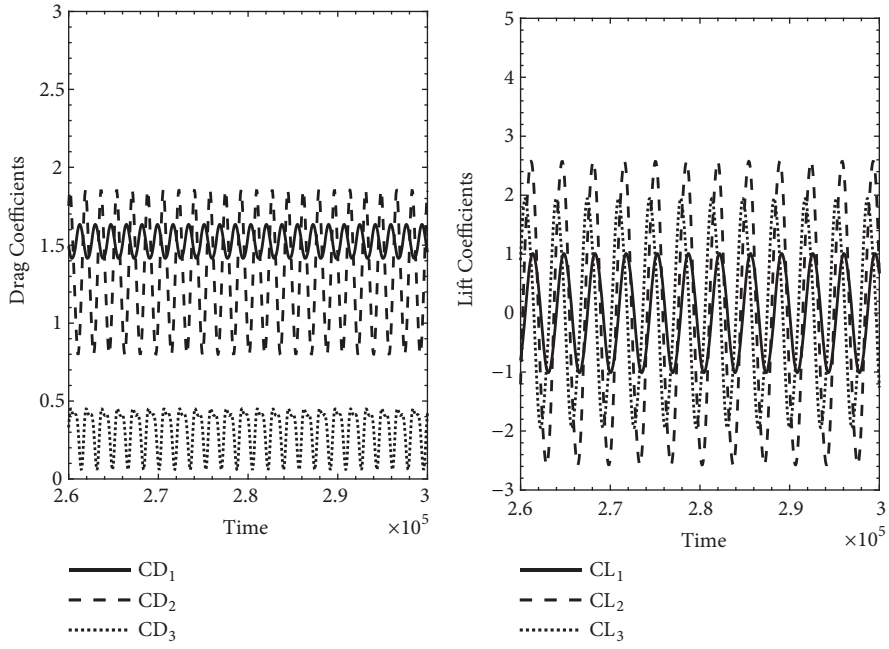

(a) Re = 200; g = 3 (b) Re = 200; g = 3

Figure 16: Temporal variation of force coefficients for alternate shedding.

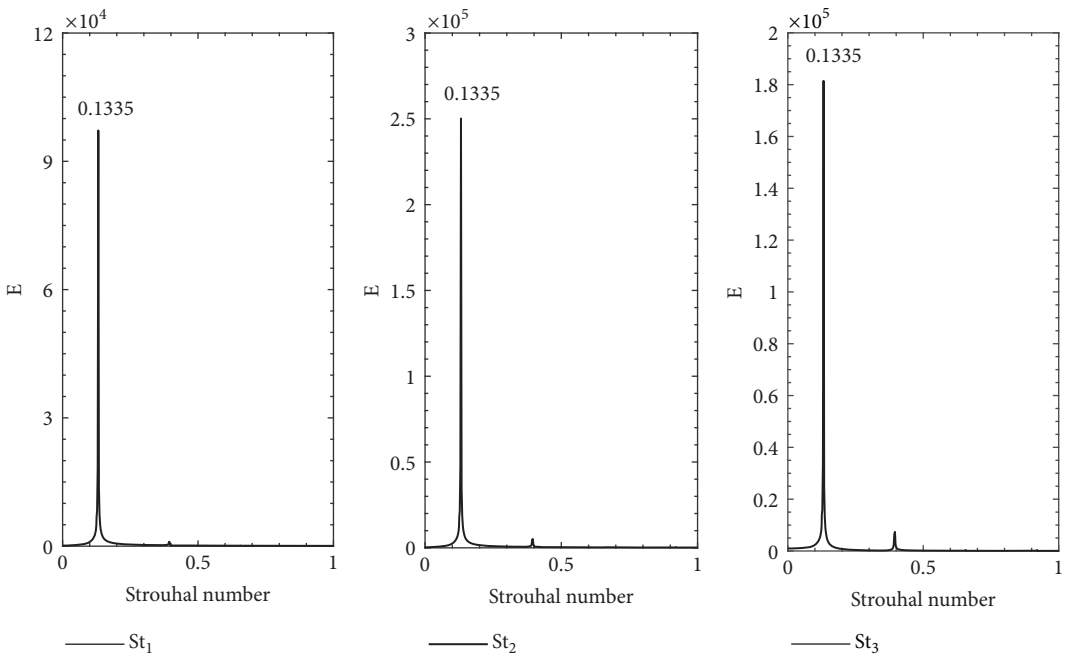

(a) Re = 200; g = 3 (b) Re = 200; g = 3 (c) Re = 200; g = 3

Figure 17: Power spectrum graph for alternate shedding.

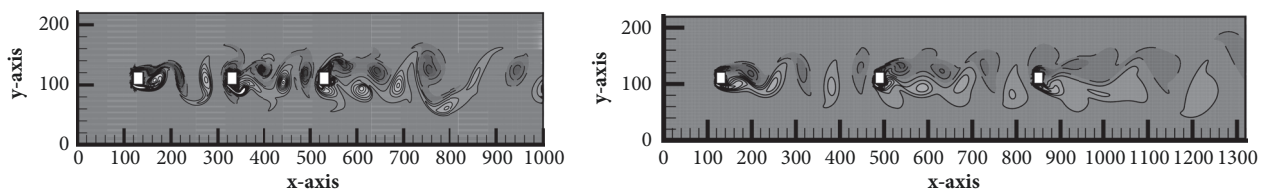

(a) Re = 200; g = 8 (b) Re = 200; g = 16

Figure 18: Vorticity contour for modulated shedding.

(a) Re = 200; g = 8 (b) Re = 200; g = 16

Figure 19: Streamlines visualization for modulated shedding.

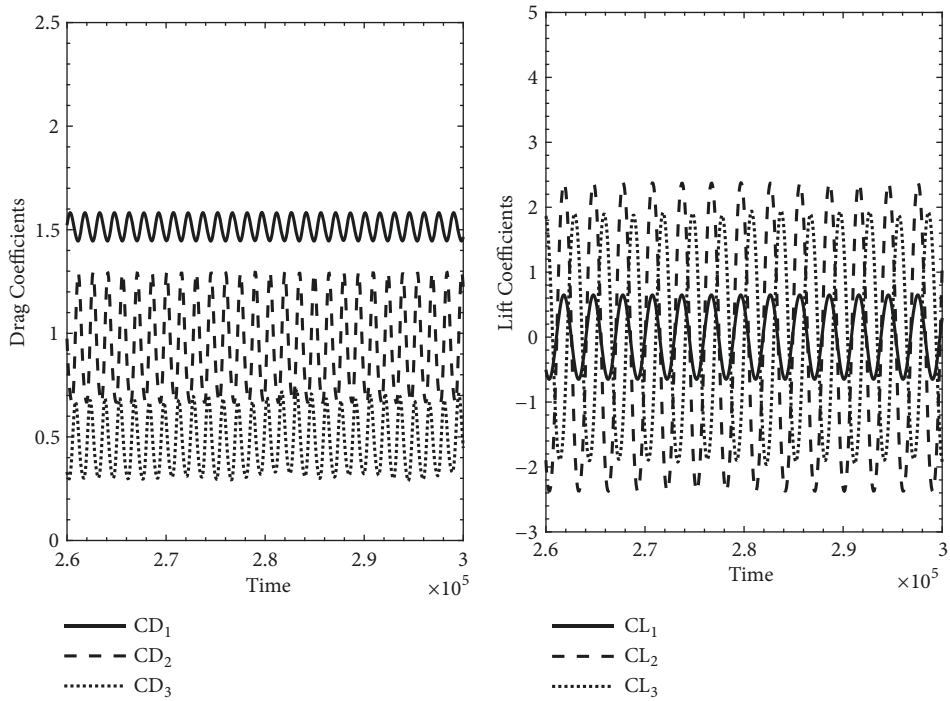

(a) Re = 200; g = 8 (b) Re = 200; g = 8

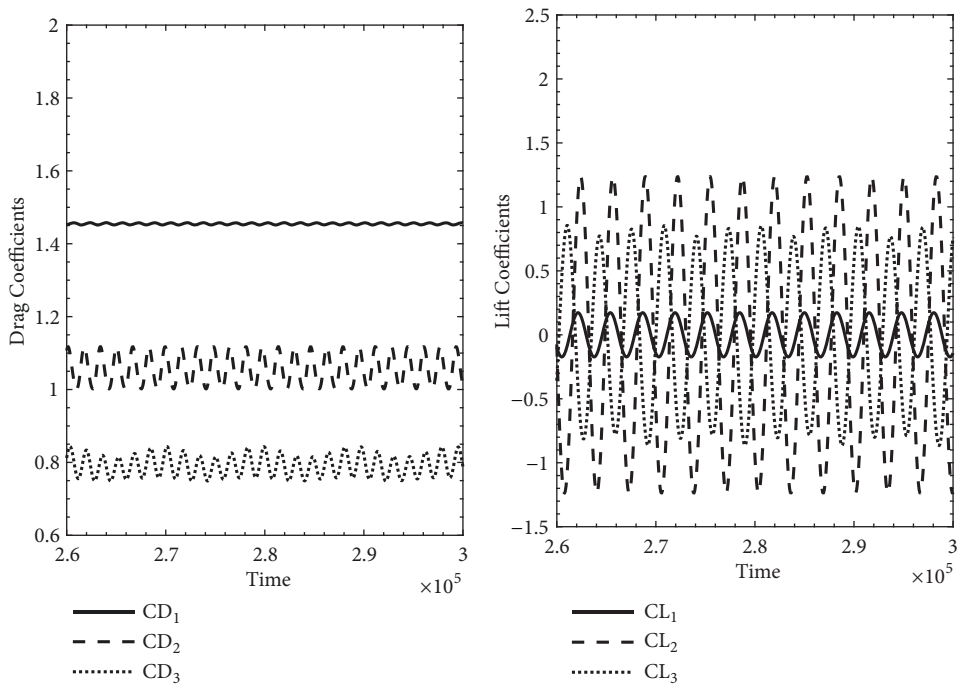

(c) Re = 200; g = 16 (d) Re = 200; g = 16

Figure 20: Temporal variation of force coefficients for modulated shedding.

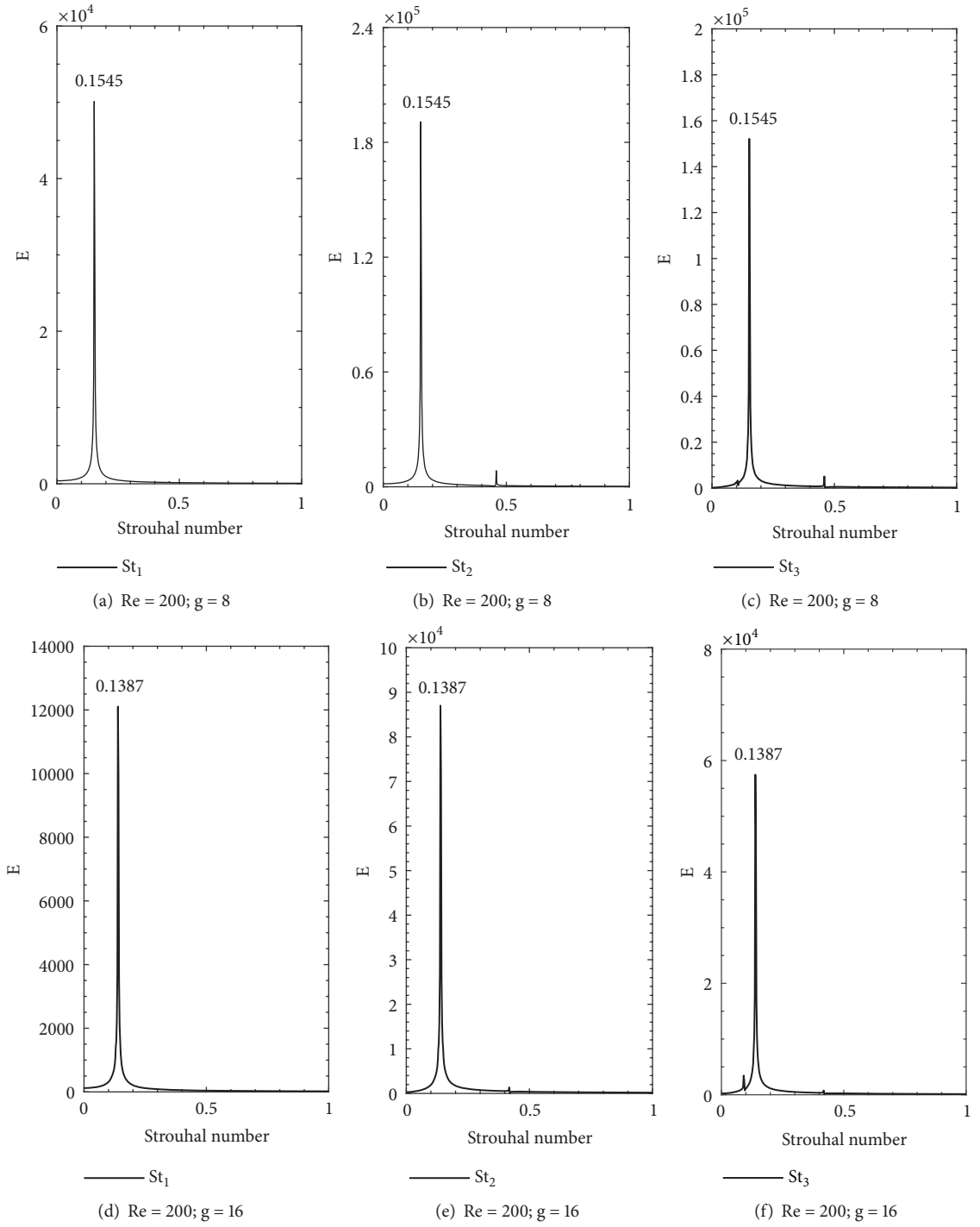

Figure 21: Power spectrum graph for modulated shedding.

Similar observations were reported by Harichandan and Roy [15] for flow around three inline circular cylinders at $Re = 100$ and 200. Further it can also be observed from Figure 23(b) that the St of all cylinders is either less or closer to the single cylinder value. Initially it shows decreasing trend and attains its local minimum value at $g = 1.5$ where gap trapped flow pattern was observed. This indicates that the vortices shed at relatively lesser frequency in the gap trapped flow pattern. In the spacing range $g = 2$ to 8 the St of all cylinders increases monotonically and coincides with single cylinder values at $g = 8$.

The RMS values of both CD and CL exhibit diverse trend and do not obey any regular pattern of increment/decrement as the gap spacing increases (Figures 23(c) and 23(d)). In the

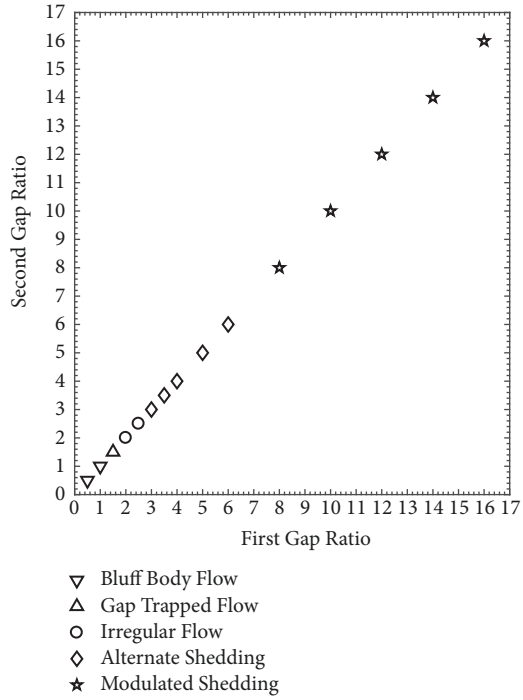

Figure 22: Flow patterns for different spacing values at $Re = 200$.

alternate shedding and modulated shedding patterns, i.e., g = 3 to 16, the RMS values of CD and CL of c_1 are closer to single cylinder values and less than both downstream cylinders. Also the RMS values of CD and CL for middle cylinder are higher than side ones in this spacing range. This might be due to regular vortex shedding from each component of triad. Further it can also be observed that the RMS values of both CD and CL are maximum at either $g = 2$ or 2.5 where irregular flow pattern was observed.

From the above discussion it can be clinched that g = 2 is the drag inversion spacing which is also termed as critical spacing. Also most of the flow parameters and flow induced forces approach their extreme values around this value. Another thing observed from above is that the flow parameters of upstream cylinder are closer to single cylinder values, but for downstream cylinders the difference confirms effect of impingement. This effect reduces with increment in spacing.

4.3. Conclusions. In this work, the numerical computations were performed in order to study the proximity effects on wake structure and flow induced forces of three inline square cylinders. The lattice Boltzmann method was used as numerical tool for this study. The spacing between cylinders was taken the same in both gaps and was systematically varied from lower to higher values in the range 0.5 to 16 diameters of cylinder. The value of Reynolds number was fixed at 200. Before analyzing the actual problem, code validation and grid independence were performed for flow around a single cylinder. Important findings of this study are listed below:

(1) Five different flow patterns were observed at different values of spacing between cylinders: bluff body flow ($0.5 \leq g \leq 1$), gap trapped flow ($g = 1.5$), irregular flow ($2 \leq g \leq 2.5$), alternate shedding ($3 \leq g \leq 6$), and modulated shedding ($8 \leq g \leq 16$).

(2) By comparison with other geometries it was found that the flow patterns for two or more than three cylinders (circular/square) may exist for the case of three inline square cylinders but within different range of spacing and Reynolds numbers.

(3) At the spacing value $g = 2$ the fluid flow characteristics changed abruptly. The drag force for middle cylinder was found to be negative in the spacing range g = 0.5 to 1.5 and it jumped to positive values at $g = 2$.

(4) The flow induced forces and shedding frequencies of first cylinder were found to be closer to those of single cylinder, but for the other two cylinders these parameters were different from single cylinder even at large values of spacing.

(5) The primary frequency, i.e., the vortex shedding frequency, was found to be dominant in all flow patterns, and the effect of secondary frequency, i.e., cylinder interaction frequency, was found to be negligible. The cylinder interaction frequencies affected the flow characteristics only in irregular flow pattern.

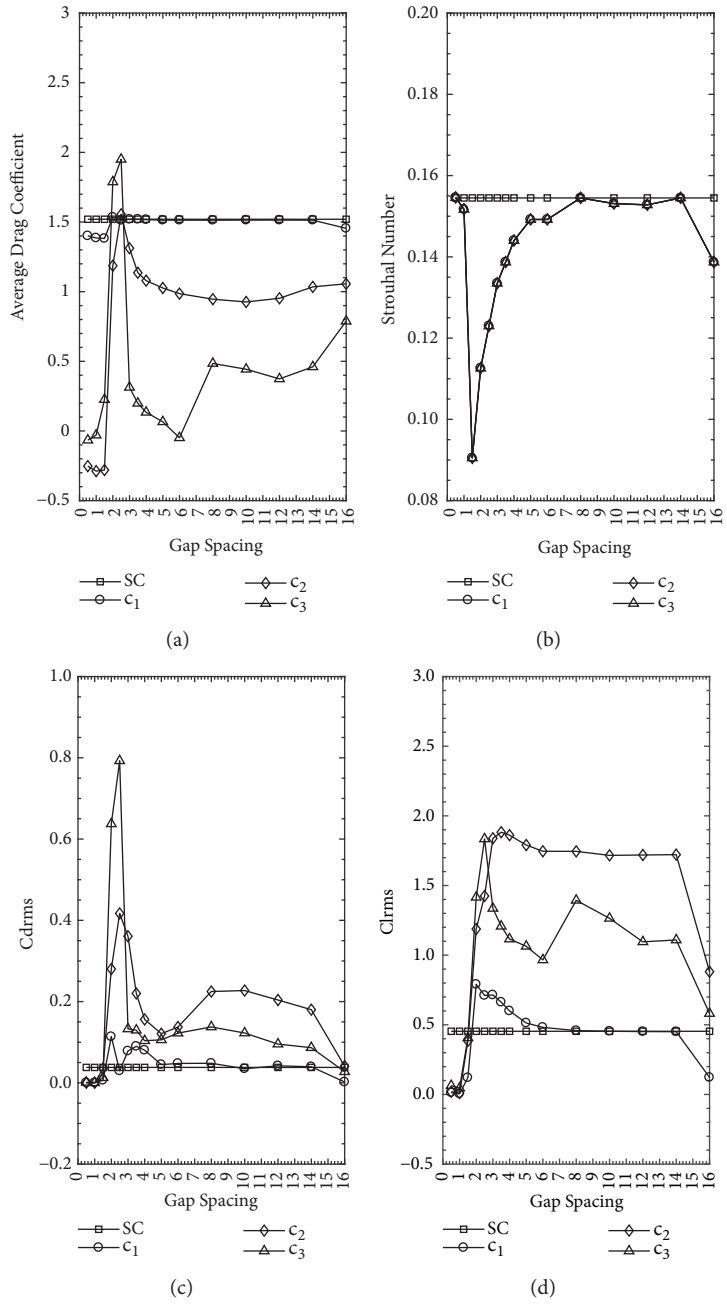

FIGURE 23: Variation of flow parameters as a function of gap spacing: (a) average drag coefficient, (b) Strouhal number, (c) root-mean-square values of drag coefficient, and (d) root-mean-square values of lift coefficient.

Data Availability

The data used to support the findings of this study are included within the article.

Conflicts of Interest

The authors declare that they have no conflicts of interest.

References

[1] M. M. Zdravkovich, "The effects of interference between circular cylinders in cross flow," *Journal of Fluids and Structures*, vol. 1, no. 2, pp. 239–261, 1987.

[2] G. Xu and Y. Zhou, "Strouhal numbers in the wake of two inline cylinders," *Experiments in Fluids*, vol. 37, pp. 248–256, 2004.

[3] T. Zheng, S. K. Tang, and B. Fei, "On the forces and strouhal numbers in the low reynolds number wakes of two cylinders in tandem," *Transactions of the Canadian Society for Mechanical Engineering*, vol. 33, no. 3, pp. 349–360, 2009.

[4] S. U. Islam, C. Y. Zhou, A. Shah, and P. Xie, "Numerical simulation of flow past rectangular cylinders with different aspect ratios using the incompressible lattice Boltzmann method," *Journal of Mechanical Science and Technology*, vol. 26, no. 4, pp. 1027–1041, 2012.

[5] S. Wang, F. Tian, L. Jia, X. Lu, and X. Yin, "Secondary vortex street in the wake of two tandem circular cylinders at low

Reynolds number," *Physical Review*, vol. 81, Article ID 036305, 2010.

[6] J. Deng, A.-L. Ren, J.-F. Zou, and X.-M. Shao, "Three-dimensional flow around two circular cylinders in tandem arrangement," *Fluid Dynamics Research*, vol. 38, pp. 386–404, 2006.

[7] Z. Han, D. Zhou, and X. Gui, "Flow past two tandem circular cylinders using Spectral element method," in *Proceedings of the Seventh International Colloquium on Bluff Body Aerodynamics and Applications (BBAA7)*, Shanghai, China, 2012.

[8] B. Sharman, F. S. Lien, L. Davidson, and C. Norberg, "Numerical predictions of low Reynolds number flows over two tandem circular cylinders," *International Journal for Numerical Methods in Fluids*, vol. 47, pp. 423–447, 2005.

[9] P. P. Patil and S. Tiwari, "Numerical investigation of laminar unsteady wakes behind two inline square cylinders confined in a channel," *Engineering Applications of Computational Fluid Mechanics*, vol. 3, no. 3, pp. 369–385, 2009.

[10] W. S. Abbasi and S. U. Islam, "Transition from steady to unsteady state flow around two inline cylinders under the effect of Reynolds numbers," *Journal of the Brazilian Society of Mechanical Sciences and Engineering*, vol. 40, no. 168, pp. 1–12, 2018.

[11] R. Franke, W. Rodi, and B. Schonung, "Numerical calculation of laminar vortex-shedding flow past cylinders," *Journal of Wind Engineering & Industrial Aerodynamics*, vol. 35, pp. 237–257, 1990.

[12] C. Norberg, "Flow around a circular cylinder: Aspects of fluctuating lift," *Journal of Fluids and Structures*, vol. 15, pp. 459–469, 2001.

[13] S. U. Islam, W. S. Abbasi, and H. Rahman, "Force statistics and wake structure mechanism of flow around a square cylinder at low Reynolds numbers," *World Academy of Science, Engineering and Technology*, vol. 8, pp. 1375–1381, 2014.

[14] A. Okajima, "Strouhal numbers of rectangular cylinders," *Journal of Fluid Mechanics*, vol. 123, pp. 379–398, 1982.

[15] A. B. Harichandan and A. Roy, "Numerical investigation of low Reynolds number flow past two and three circular cylinders using unstructured grid CFR scheme," *International Journal of Heat and Fluid Flow*, vol. 31, pp. 154–171, 2010.

[16] M. K. Kim, D. K. Kim, S. H. Yoon, and D. H. Lee, "Measurements of the flow fields around two square cylinders in a tandem arrangement," *Journal of Mechanical Science and Technology*, vol. 22, pp. 397–407, 2008.

[17] C.-H. Liu and J. M. Chen, "Observations of hysteresis in flow around two square cylinders in a tandem arrangement," *Journal of Wind Engineering & Industrial Aerodynamics*, vol. 90, no. 9, pp. 1019–1050, 2002.

[18] H. Sakamoto, H. Haniu, and Y. Obata, "Fluctuating forces acting on two square prisms in a tandem arrangement," *Journal of Wind Engineering & Industrial Aerodynamics*, vol. 26, pp. 85–103, 1987.

[19] A. T. Sayers, "Flow interference between four equispaced cylinders when subjected to a cross flow," *Journal of Wind Engineering & Industrial Aerodynamics*, vol. 31, no. 1, pp. 9–28, 1988.

[20] K. Lam and S. C. Lo, "A visualization study of cross-flow around four cylinders in a square configuration," *Journal of Fluids and Structure*, vol. 6, pp. 109–131, 1992.

[21] O. Inoue, M. Mori, and N. Hatakeyama, "Aeolian tones radiated from flow past two square cylinders in tandem," *Physics of Fluids*, vol. 18, no. 4, Article ID 046101, 2006.

[22] A. Etminan, "Flow and heat transfer over two bluff bodies from very low to high Reynolds numbers in the laminar and turbulent flow regimes," *International Journal of Advanced Manufacturing Technology*, vol. 6, no. 2, pp. 61–72, 2013.

[23] Y. Bao, Q. Wu, and D. Zhou, "Numerical investigation of flow around an inline square cylinder array with different spacing ratios," *Computers & Fluids*, vol. 55, pp. 118–131, 2012.

[24] S. U. Islam, W. S. Abbasi, and Z. C. Ying, "Transitions in the unsteady wakes and aerodynamic characteristics of the flow past three square cylinders aligned inline," *Aerospace Science and Technology*, vol. 50, pp. 96–111, 2016.

[25] Y. Gao, C. Yin, H. Zhang, K. Yang, X. Zhao, and Z. Sun, "Numerical study on flow around four square-arranged cylinders at low Reynolds numbers," *Mathematical Problems in Engineering*, vol. 2017, Article ID 6381256, 18 pages, 2017.

[26] W. S. Abbasi, S. U. Islam, H. Rahman, and R. Manzoor, "Numerical investigation of fluid-solid interaction for flow around three square cylinders," *AIP Advances*, vol. 8, Article ID 025221, pp. 1–16, 2018.

[27] U. Frisch, B. Hasslacher, and Y. Pomeau, "Lattice-gas automata for the Navier-Stokes equation," *Physical Review Letters*, vol. 56, no. 14, pp. 1505–1508, 1986.

[28] G. R. McNamara and G. Zanetti, "Use of the boltzmann equation to simulate lattice-gas automata," *Physical Review Letters*, vol. 61, no. 20, pp. 2332–2335, 1988.

[29] P. L. Bhatnagar, E. P. Gross, and M. Krook, "A model for collision processes in gases. I. Small amplitude processes in charged and neutral one-component systems," *Physical Review*, vol. 94, no. 3, pp. 511–525, 1954.

[30] A. A. Mohamad, *Lattice Boltzmann Method: Fundamentals and Engineering Applications with Computer Codes*, Springer, 2011.

[31] D. A. Wolf-Gladrow, *Lattice-Gas Cellular Automata and Lattice Boltzmann Models-An introduction*, Springer, 2005.

[32] Z. Guo, H. Liu, L.-S. Luo, and K. Xu, "A comparative study of the LBE and GKS methods for 2D near incompressible laminar flows," *Journal of Computational Physics*, vol. 227, pp. 4955–4976, 2008.

[33] M. A. Gallivan, D. R. Noble, J. G. Georgiadis, and R. O. Buckius, "An evaluation of the bounce-back boundary condition for lattice Boltzmann simulations," *International Journal for Numerical Methods in Fluids*, vol. 25, no. 3, pp. 249–263, 1997.

[34] T. Igarashi and K. Suzuki, "Characteristics of the flow around three circular cylinders arranged inline," *Bulletin of the JSME*, vol. 27, no. 233, pp. 2397–2404, 1984.

[35] A. A. Hetz, M. N. Dhaubhadel, and D. P. Telionis, "Vortex shedding over five in-line cylinders," *Journal of Fluids and Structures*, vol. 5, no. 3, pp. 243–257, 1991.

[36] C. M. Sewatkar, R. Patel, A. Sharma, and A. Agrawal, "Flow around six in-line square cylinders," *Journal of Fluid Mechanics*, vol. 710, pp. 195–233, 2012.